JOURNAL OF MATERIALS SCIENCE 26 (1991) 4897–4904

Kinetics of the oxidative degradation of ceramic injection-moulding vehicle

J. K. WRIGHT*, J. R. G. EVANS
Department of Materials Technology, Brunel University, Uxbridge, Middlesex UB8 3PH, UK

The effective reaction depth during the pyrolysis of ceramic injection-moulded bodies in oxidizing atmospheres was deduced from isothermal thermogravimetry. The kinetic data were analysed (i) for the case of chemical reaction control, (ii) for mass transport control and (iii) for combined chemical and mass transport control. The shrinking core reaction modulus indicates that reaction rate was mainly controlled by the diffusion of oxygen into the surface region and degradation products out. The results are used to discuss the relative merits of oxidative and thermal degradation of organic vehicle for ceramic processing.

1. Introduction

There is considerable interest in the production of technical ceramic components by injection-moulding [1, 2]. The ceramic powder is incorporated in an organic vehicle which enables the resulting suspension to be fabricated by plastic forming operations. After shaping, the organic vehicle must be removed from the ceramic powder assembly without disrupting the particle arrangement. Polyolefins in the form of waxes and high polymers have been widely used as components for the organic vehicle [3–7] and have been removed by pyrolysis from the ceramic body.

During the pyrolytic degradation of polyolefins, two reaction routes may precede the evaporation of degradation products: oxidative and thermal degradation. During the oxidative degradation of polyethylene, the primary process is one of hydroperoxidation [8]. The hydroperoxide group is important in the induction period of degradation, acting as a precursor for other oxygen-containing degradation products and promoting the autocatalytic reaction sequence.

The presence of hydroperoxide groups, however, is dependent on a continuous supply of oxygen. It follows that the extent of oxidative degradation in a large section is controlled by the depth of oxygen diffusion from the surface. In contrast, thermal degradation of the polymer by free-radical reactions takes place were there is no available oxygen [9]. Volatile fragments are created at all points throughout the body and such fragments may be lost by diffusion to the surface followed by evaporation. In large bodies, mass transport by diffusion is limited and internal voids may result from the boiling of degradation products.

The internal thermal degradation reaction is a high activation energy process with values in the region of 193–227 kJ mol^{-1} [10]. Oxidative degradation, on the other hand, is a lower activation energy process involving 30–40 kJ mol^{-1} [11] and thus tends to predominate at lower temperatures. When the suspension contains low molecular weight species such as waxes or stearic acid, weight loss occurs by evaporation without chain scission and is independent of the ambient atmosphere [11].

Previous work [11] showed that in ceramic injection-moulding suspensions based on polyethylenes, dynamic thermogravimetry in an oxidizing atmosphere revealed a strong dependence of weight loss on sample size, and this was explained by oxygen diffusion control.

The purpose of the present work was to assess the extent of oxidative degradation on the removal of polyethylene from a ceramic injection-moulding suspension incorporating a fine alumina powder, by studying the kinetics of the shrinking unreacted core reaction. This issue has several important practical consequences. In the first place, if the thermal degradation reactions could be controlled by, for example, employing low temperatures or high oxygen partial pressures, then it might be possible to secure complete removal of the organic vehicle by a shrinking reaction interface process involving oxidative degradation. This would avoid the deleterious effect of volatile degradation products of thermal degradation deep inside the suspension. In the second place, it has been shown that there is a slight volumetric shrinkage of the powder assembly as the organic vehicle departs from particle junctions [12]. Once the effective volume fraction of the ceramic reaches a critical value as a result of the loss of organic vehicle, fluid properties are lost and the suspension behaves as a brittle solid [12]. Thus, if a surface layer is rapidly depleted of vehicle in advance of the core, shrinkage will be non-uniform and defects may result [13].

2. Experimental procedure

2.1. Preparation of the suspension

Details of the composition are given in Table I. Stearic acid was added to the mixture to act as a lubricant

Present address: Department of Agricultural and Forest Sciences, University College of North Wales, Bangor, Gwynedd, UK.

0022–2461/91 $03.00 + .12

TABLE I Materials and composition of the formulation

Material	Density ($kg\ m^{-3}$)	Grade/company	Content[a] (wt %)	Content (vol %)
Alumina	3987	A16SG Alcoa GB Ltd	86.33	59.5
Low-density polyethylene[b]	926	Escorene LD657 Esso UK	11.67	34.7

[a] 2 wt % of stearic acid was added to the formulation as a processing aid.
[b] Molecular weight M_n = 8000, determined by gel permeation chromatography at RAPRA Laboratories, Shrewsbury, UK.

[14], to reduce the uptake of iron from the compounding machinery and to limit the mechanical degradation of polyethylene induced by high-shear mixing at a solids loading of 60 vol %. Details of the exact composition are given in Table I and are based on the average of four ashing results.

The alumina powder and organic components were mixed in a Henschel high-speed mixer, using a procedure described previously [11], to give an approximate volume loading of 60 vol % ceramic. Compounding was performed using a twin-screw extruder model TS40 (Betol Machinery, Luton, UK), the operation of which has been previously described [15]. The barrel temperature profile (feed to exit) was 130–190–200–195 °C. The extrudate was then water-cooled, dried and granulated.

Samples were then compression-moulded at a temperature of 145 °C and at a pressure of 12 MPa in an Apex M1/R hydraulic press. Samples prepared were of 18 mm diameter, and of thicknesses 0.5, 0.75, 1.0 and 2.0 mm. Discs of thickness 4 mm and radius 31 mm were also prepared.

2.2. Thermogravimetric analysis

A Stanton thermobalance (model TR02) was used for thermogravimetric analysis under flowing air and nitrogen, the flow rate in both cases being $40\ l\ h^{-1}$. Isothermal experiments were carried out at 180 °C on both the moulded samples and powdered material. This temperature was selected to provide significant weight loss in the time-scale used, whilst being low enough to prevent the excessive bloating or cracking which can be caused by higher temperatures. A minimum of four samples were run in each atmosphere at each thickness with the exception of the 4 mm samples, where only two were run in each atmosphere. The curves for each condition were averaged. The shrinking core reaction modulus and effective diffusivities for the moulded samples were calculated by the method of Szekely *et al* [16].

3. Results and discussion

3.1. Interpretation of thermogravimetric curves

Figs 1 and 2 show the results of the isothermal thermogravimetric analysis experiments for the five thicknesses of sample in flowing air and flowing nitrogen, respectively. Fig. 3 shows the corresponding

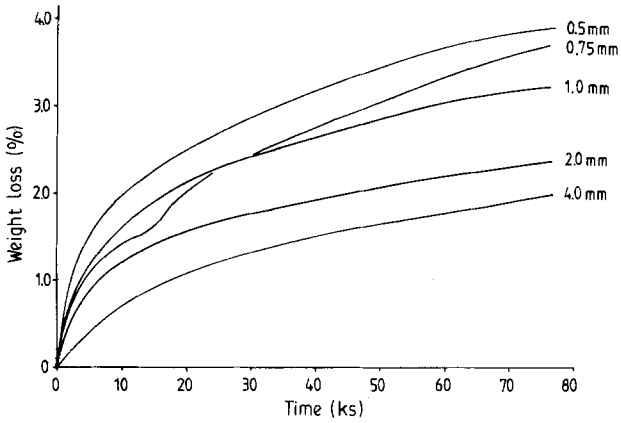

Figure 1 Isothermal weight-loss fraction based on initial total weight for compression-moulded discs of various thickness in flowing air (smoothed curves).

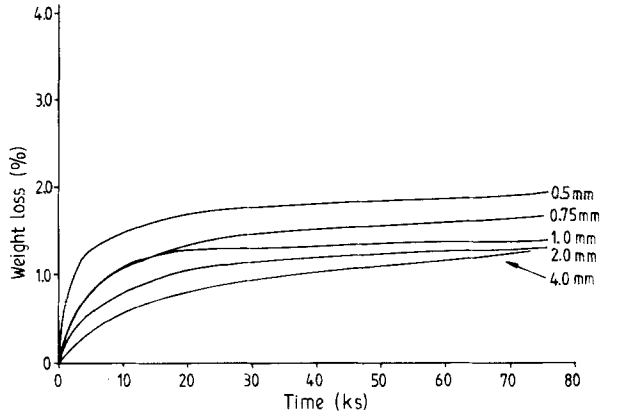

Figure 2 Isothermal weight-loss fraction based on initial total weight for compression-moulded discs of various thickness in flowing nitrogen (smoothed curves).

weight-loss curves for material which had been finely ground in a pestle and mortar, for which diffusion effects are considered to be negligible. This curve therefore reveals the kinetics of reaction which for polyethylene is a first-order process [17] given by

$$\frac{dw}{dt} = -k(w_0 - w) \quad (1)$$

where w is the weight loss of reactant and k is the rate constant at the temperature under consideration. For a ceramic suspension of ceramic weight fraction m_c the

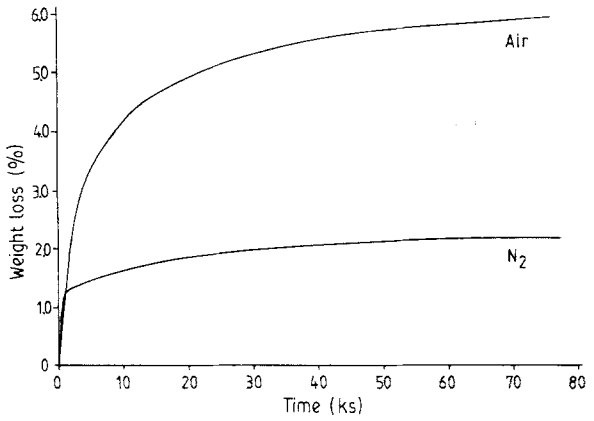

Figure 3 Isothermal weight-loss fraction based on initial total weight for powdered ceramic moulding suspension in flowing air and nitrogen (smoothed curves).

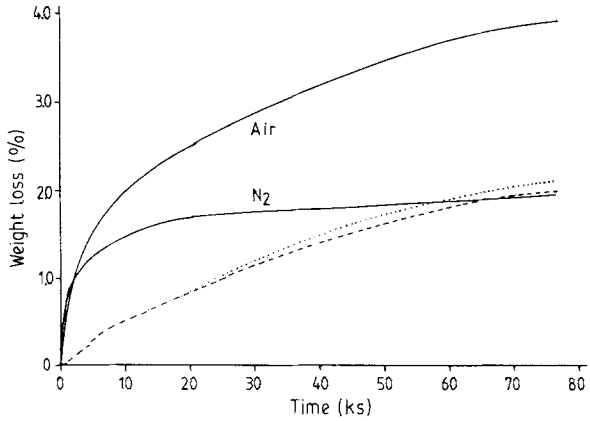

Figure 4 Isothermal curves for the 0.5 mm discs in air and nitrogen together with (– – –) the subtracted curve and (. . .) the corrected subtraction.

initial weight of reactant is

$$w_0 = W_0(1 - m_c) \quad (2)$$

where W_0 is the initial sample weight.

The separation of weight loss due to thermal degradation in the interior of the discs from weight loss caused by oxidative reaction at the surface presents a problem. It is clear that at 180 °C both processes are operative. Fig. 2 shows the weight loss observed in a nitrogen atmosphere, indicating a dependence on sample thickness because of the limiting effect of outward diffusion of degradation products and stearic acid through the suspension. In the less sensitive dynamic thermogram [11] this effect is not easily detected, the evolution of degradation products being so rapid that it causes cracks which effectively reduce the sample size. In order to determine the weight loss associated with oxidative degradation at each thickness, the weight loss curve obtained in nitrogen was subtracted from the weight loss curve obtained in air:

$$\left(\frac{w}{W_0}\right)_{O_2} = \left(\frac{w}{W_0}\right)_{air} - \left(\frac{w}{W_0}\right)_{N_2} \quad (3)$$

giving a separate curve for each sample thickness based on the initial total sample weight, W_0, which includes the ceramic powder.

This procedure introduces an error which is most pronounced in the thinnest sample, since reactant which is decomposed by oxidative degradation cannot also be responsible for weight loss by thermal degradation. A correction for this error is described below.

Since the samples were in the form of thin discs, the total area A of each sample (neglecting the area of the rim) was known. The samples were supported on coarse stainless steel mesh, allowing the reaction to take place at both sides. The volume of polymer lost per unit area could be found at each time interval from

$$\left(\frac{V}{A}\right)_{O_2} = \left(\frac{w}{W_0}\right)_{O_2} \frac{W_0}{A\rho} \quad (4)$$

where ρ is the density of the polymer fraction which was 928 kg m^{-3}, assuming that the individual organic components present their own density when mixed.

If V_p is the volume fraction of polymer in the suspension then the absolute reaction depth, x, can be obtained and expressed as a fraction of the half thickness, y, following the procedure of Szekely *et al.* [16]

$$X = \frac{x}{y} = \frac{1}{y}\left(\frac{V}{A}\right)_{O_2} \frac{1}{V_p} \quad (5)$$

noting that $W_0/yA\rho V_p$ is the reciprocal of weight fraction of polymer in the suspension at the start. Once the depth of the reaction interface is known, a correction can be made for the error caused by subtraction. This was applied to the thinnest sample to show the maximum error. From the reaction depth at time t, the original mass of material in the reaction layer was obtained. Using data from Fig. 3, the loss in nitrogen directly caused by the mass of material in the reaction layer was found. This was converted to a weight fraction based on the original mass of the sample and added to the right-hand side of Equation 3. The results of this exercise are shown in Fig. 4, from which it can be seen that the correction is so small as to be insignificant, even for the thinnest sample.

3.2. Analysis of reaction kinetics where chemical reaction is rate-controlling

Although the polymer is a liquid, the ceramic suspension maintains its form as a result of the high solids loading and the extent of reaction can be treated according to the kinetics of gas–solid reactions.

This approach has been successfully applied to the oxidation of graphite in ceramic–graphite composites [18, 19] which is an analogous problem. The kinetics of reaction can be analysed assuming that either chemical reaction or mass transport controls the rate, or according to combined reaction and diffusion control.

Szekely *et al.* [16] consider the kinetics of a reaction of the type

$$A(g) + bB(s) = cC(g) + dD(s) \quad (6)$$

where gaseous products are displaced and a reaction-product layer forms. For infinitely flat plates under conditions where the irreversible reaction controls the

rate, the reaction depth X is a linear function of time t:

$$X = \frac{bK_1[O_2]}{\rho_s y} t \quad (7)$$

where K_1 is a first-order rate constant for a rate expressed as moles of gaseous reactant per unit time per unit area; K_1 therefore has units (m s^{-1}). ρ_s is the molar density of the solid reactant B and the molar oxygen concentration in the gas stream is $[O_2]$.

For the reaction

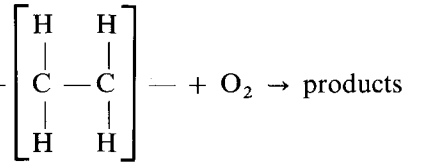

Meltzer *et al.* [20] report oxygen uptake data in the region 140–170 °C under conditions where the polyethylene was in the form of a thin supported film to minimize the effect of oxygen diffusion control. Since the maximum uptakes were 0.6 m^3 kg^{-1} at 166 °C, b can be taken as 1.46.

Inspection of Fig. 5 shows that the curves of X against t are not perfectly linear, but taking slopes for reaction times in the region of 20–70 ks values of K_1 may be estimated (Table II). The concentration of oxygen was taken as 5.4 mol m^{-3} at 453 K and the density of the reactant was taken as the molar density of polyethylene multiplied by the volume fraction of polyethylene in the body, giving 11 575 mol m^{-3}. This is an effective density for polyethylene based on the total volume, and gives a rate constant for the reaction of polyethylene in this suspension.

The shrinking unreacted core model is valid for bodies whose overall size does not change during the reaction. In fact ceramic bodies undergo a shrinkage as organic matter is removed from particle junctions. However, in oxidizing atmospheres this shrinkage is low (~ 1% linear) and the overall size of the body can be regarded as constant [12].

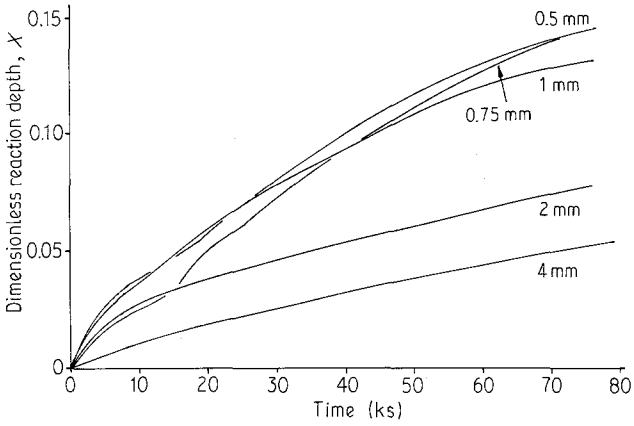

Figure 5 Dimensionless reaction depth as a function of time (smoothed curves).

TABLE II Rate constant assuming reaction control deduced from Fig. 5 and effective diffusion coefficient assuming mass transport control deduced from Fig. 6

Sample half-thickness, y (mm)	Rate constant, K_1 (m s^{-1})	Effective diffusion coefficient, D_e (m^2 s^{-1})
0.25	0.6×10^{-6}	1.6×10^{-11}
0.375	1.0×10^{-6}	3.8×10^{-11}
0.5	1.0×10^{-6}	5.1×10^{-11}
1.0	1.1×10^{-6}	6.3×10^{-11}
2.0	1.8×10^{-6}	13.1×10^{-11}

3.3. Analysis of reaction kinetics where diffusion controls the rate

The fact that linear plots are not obtained in Fig. 5 shows that diffusion also controls the rate of weight loss. Szekely *et al.* [16] give an expression for the extent of irreversible reaction for a flat plate under conditions of diffusion control:

$$X^2 = \frac{2b[O_2]D_e}{\rho_s y^2} t \quad (8)$$

where D_e is the effective diffusion coefficient.

The experimental data are replotted as X^2 against t in Fig. 6 and it can be seen that pronounced diffusion control is evidenced after 20 ks by the straight lines. Values of D_e, obtained from these lines (neglecting the time period 0–20 ks, where experimental error is enlarged by subtraction of measurements of small weight loss) are given in Table II. The physical interpretation of these coefficients requires considerable care. They represent not only the inward diffusion of reactant. Since the extent of reaction is assessed by weight loss which includes the exodus of degradation products, these in turn must diffuse through the polymer in the interstitial pore space.

3.4. Combined reaction and diffusion control

Szekely *et al.* [16] also give an expression for the extent of reaction X as a function of dimensionless time τ and reaction modulus σ_s^2 for the case where chemical reaction at the interface between the shrinking core and the gaseous phase as well as diffusion

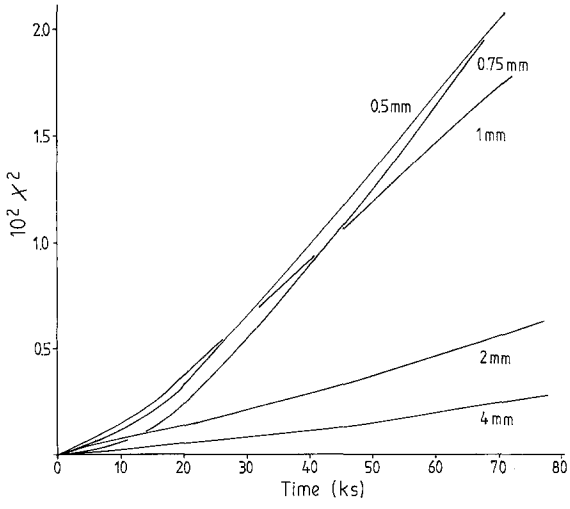

Figure 6 Square of dimensionless reaction depth as a function of time (smoothed curves).

through a boundary layer determine the overall rates:

$$t = \tau g_{F_p}(X) + \sigma_s^2 \tau P_{F_p}(X) \quad (9)$$

where $g_{F_p}(X) = 1 - (1 - X)^{1/F_p}$ and F_p is the shape factor having values 1, 2 and 3 for flat plates, cylinders and spheres, respectively. Thus for a flat plate [16]

$$g_{F_p}(X) = X$$
$$P_{F_p}(X) = X^2 \quad (10)$$

and σ_s^2 is the shrinking core reaction modulus. $P_{F_p}(X)$ is a conversion function dependent on geometry.

Equation 9 may be rewritten as

$$t = \tau X + \tau \sigma_s^2 X^2 \quad (11)$$

from which τ and σ_s^2 can be obtained by plotting t/X as a function of X, giving τ as intercept and $\tau\sigma_s^2$ as gradient. The value of σ_s^2 reveals the extent of diffusional or chemical reaction control. When σ_s^2 is smaller than 0.1 the rate of reaction can be considered to be controlled entirely by chemical reaction. Alternatively, when σ_s^2 is larger than 10 the rate is controlled by diffusion through the product layer and by external mass transfer [16]. The maximum deviation from entire control by either extreme occurs when $\sigma_s^2 = 1$, and these criteria are general regardless of geometry. Data points obtained from the curves in Fig. 5 representing times greater than 20 ks were plotted as T/X against X in Fig. 7, and linear regression analysis produced values of σ_s^2 and τ which are given in Table III. The values of σ_s^2 are all greater than unity, indicating that the rate of weight loss was mainly controlled by diffusion in the presence of an oxygen-rich atmosphere. The results for the 4 mm discs, which are not plotted in Fig. 7, suggest a high rate constant and effective diffusivity. This is because 4 mm discs all cracked during isothermal heat treatment at 180 °C (Fig. 8), exposing extra reaction surface.

The constant τ is related to the rate constant for an irreversible reaction in an infinite flat plate by Equation 3.2.5 in Szekely *et al.* [16]:

$$\frac{1}{\tau} = \frac{b K_1 [O_2]}{\rho_s y} \quad (12)$$

from which values of rate constant derived from the combined reaction–mass-transport model are given in Table III, and as expected are slightly higher than those obtained from the assumption that chemical reaction was rate controlling or that $D_e = \infty$ ($\sigma_s^2 = 0$ in Equation 11).

Furthermore, the effective diffusion coefficient D_e for diffusion through the reaction product layer can be obtained from [16]

$$\sigma_s^2 = \frac{K_1}{2D_e}\left(\frac{V}{A}\right)\left(1 + \frac{1}{K_e}\right) \quad (13)$$

where K_e is the equilibrium constant for the reaction,

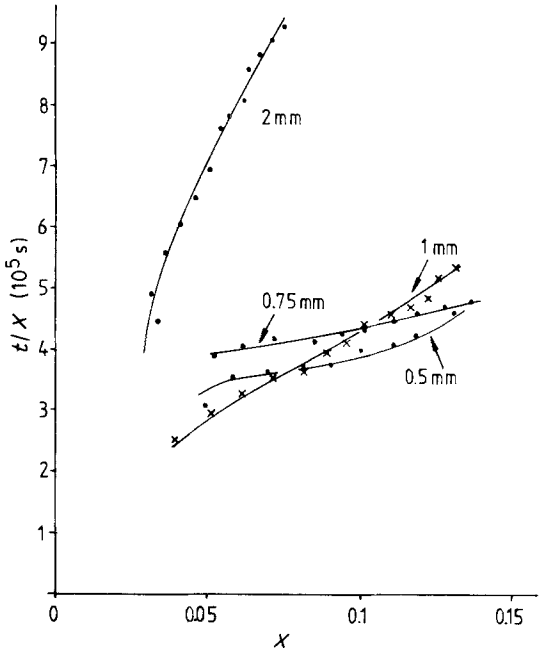

Figure 7 t/X as a function of X from which rate constant and reaction modulus are obtained.

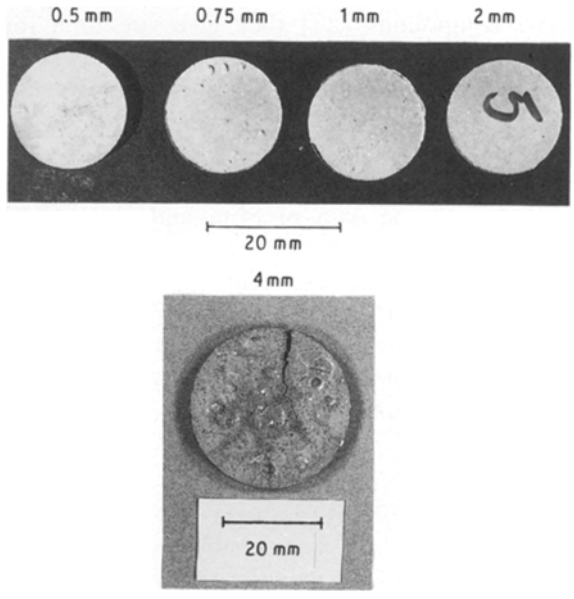

Figure 8 Appearance of the discs after heat treatment.

TABLE III Shrinking core reaction modulus, together with chemical rate constant and effective diffusion coefficient

Sample half-thickness, y (mm)	Shrinking core reaction modulus, σ_s^2	τ (ks)	K_1 (m s^{-1})	D_e (m^2 s^{-1})
0.25	6.9	239	1.5×10^{-6}	2.7×10^{-11}
0.375	3.0	336	1.6×10^{-6}	10.0×10^{-11}
0.5	18.8	149	4.9×10^{-6}	6.5×10^{-11}
1.0	43.5	221	6.6×10^{-6}	7.6×10^{-11}
2.0	13.4	835	3.5×10^{-6}	26×10^{-11}

from which

$$D_e = \frac{K_1 y}{2\sigma_s^2}$$

a result which is obtained by comparing Equations 8, 11 and 12 for the case where X is proportional to $t^{1/2}$. V and A are the volume and surface area of the disc; K_e is taken to be infinite for an irreversible reaction so that the term $1/K_e$ can be neglected.

Values for effective diffusion coefficient can be found and are given in Table III. These are all of the same order of magnitude as those in Table II but are higher than values obtained from the assumption that diffusion exclusively controls the rate of weight loss. The interpretation of the physical significance of these values does, however, require some consideration. Mita and Horie [21] give values for the activation energy and the pre-exponential coefficient for the diffusion of oxygen in polyethylene as 38–40 kJ mol^{-1} and 2.0–4.5 $\times 10^{-4}$ m^2 s^{-1}, respectively, from which the diffusivity at 180 °C is 4.9×10^{-9} to 1.9×10^{-8} m^2 s^{-1}. These values are obtained below the melting point and therefore reflect diffusion in the amorphous fraction. Nevertheless, the effective diffusion coefficient here is three orders of magnitude lower, and it is difficult to imagine that it reflects oxygen diffusion. D_e is estimated from weight loss measurements where the overall process involves an ingress of oxygen and the exit of reaction products. Thus the latter process may control the rate, and since the diffusing species include larger molecules than oxygen such as acids, peroxide compounds and carbonyl compounds [22] they give rise to a lower effective diffusion coefficient. Some support for this view is obtained from the observation that the surface of some samples showed blistering (Fig. 8) caused by the impediment to mass transport of outward-moving degradation products. Furthermore, a direct comparison with the data of Mita and Horie [21] is impeded by the fact that diffusion in the suspension is limited by the presence of ceramic powder. A number of mass transport laws for particle-filled composites have been proposed [23–25], but few have been validated by experiments under conditions relevant to the pyrolysis of ceramic moulded bodies.

3.5. Completion of reaction

If chemical reaction is rate-controlling then the time for completion of the oxidative reaction $t_{x=1}$ can be found from [16]

$$t_{x=1} = \frac{\rho_s y}{b K_1 [O_2]} \quad (14)$$

These times are given in Table IV based on the values of K_1 in Table II. Clearly, complete removal of organic vehicle from a ceramic body would be a lengthy process under the isothermal conditions selected. However, $t_{x=1}$ is underestimated by Equation 14 because the curves in Fig. 5 are not linear. A value of $t_{x=1}$ can be obtained from the assumption that mass transport controls rate of reaction from Equation 8:

$$t_{x=1} = \frac{y^2 \rho_s}{2b[O_2]D_e} \quad (15)$$

These times are also shown in Table IV and are obviously considerably longer.

Another estimate of completion time for the oxidative reaction for the case of mixed reaction and diffusion control can be obtained from Equation 11 by putting $X = 1$. The values thus obtained are also given in Table IV for comparison.

3.6. Competition between surface oxidation and through-thickness thermal degradation

The complete removal of organic vehicle by a shrinking unreacted core process in an oxidizing atmosphere would require careful control of the competition between oxidative and thermal degradation. The rate constants under both conditions obtained from the dynamic thermograms in previous work [11] for the composition used here are shown in Fig. 9. These are reaction rate constants for the complete weight-loss process including evaporation of stearic acid. Clearly at low temperatures the oxidative reaction predominates. The effect is emphasized in Fig. 10, where the ratio $K_{oxid}/K_{thermal}$ is plotted as a function of temperature. At low temperatures, the oxidative reaction dominates but is slow as shown by the values for $t_{x=1}$ in Table IV. Furthermore, thermal degradation is never completely eliminated. A polymer intended for removal entirely by oxidative processes would require a very large disparity between the energy required to break the backbone in the presence and absence of oxidation. In the present example, C–C bond breakage, which contributes to chain scission and hence production of volatilizable fragments, requires an energy of 290 kJ mol^{-1} under thermal

TABLE IV Predicted times for isothermal completion of the oxidative reaction

Sample half-thickness (mm)	Assuming reaction control		Assuming diffusion control		Combined reaction and diffusion control	
	(ks)	(days)	(ks)	(days)	(ks)	(days)
0.25	612	7.1	2867	33	1888	22
0.375	551	6.4	2717	31	1344	16
0.5	667	7.7	3598	42	2950	34
1.0	1335	15	11652	135	9835	114
2.0	1631	18.8	22414	259	12024	139

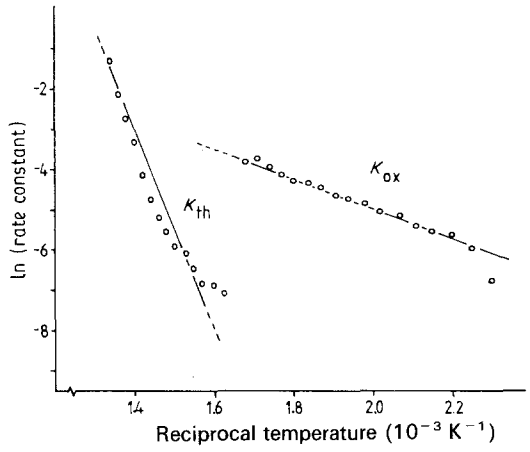

Figure 9 Activation energy plots for fine powdered material under either oxidative or thermal degradation.

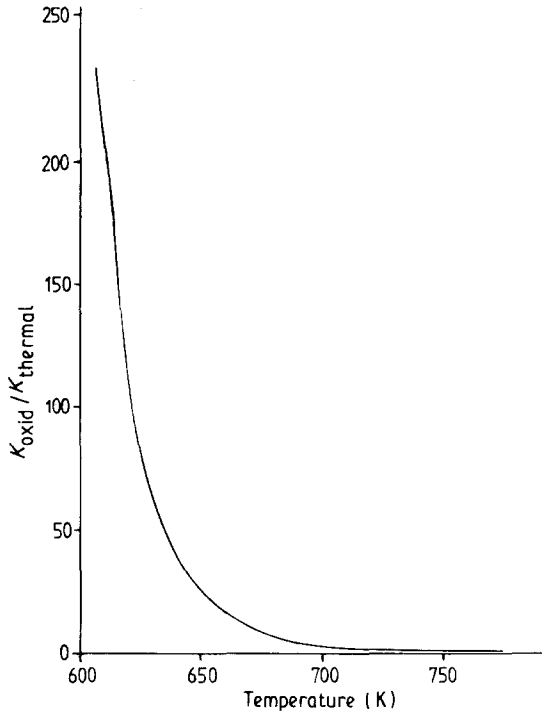

Figure 10 Ratio of oxidative to thermal degradation rates as a function of temperature.

degradation conditions [26], whereas in the presence of oxidation this is reduced to 130 kJ mol^{-1} [22].

There is, however, a further problem with this approach. If the effective diffusivity measured here is related to the exit of degradation products through a product layer rather than the ingress of oxygen, then a low-temperature extended heat treatment may result in a greater oxygen uptake deeper into the body, and the surface-specific reaction which is apparently desirable would not be obtained. Such a situation would be less favourable than thermal degradation because at lower temperatures diffusion in the polymer melt would be slower and there would be a greater likelihood of blistering or bloating.

The main weakness of the application of the shrinking core reaction model to polymers which undergo an autooxidation reaction sequence is that the reaction path may itself be dependent on oxygen activity [27]. Thus at low partial pressure of oxygen the reaction of radicals to form inert products is favoured. However, it is reported that for polyethylene in the temperature range 140–170 °C the oxidation rate is directly proportional to oxygen partial pressure in the range 6.9–188 kPa [28]. This proportionality is commensurate with the rate equation (Equation 3.2.1 in Szekely *et al.* [16]) upon which the shrinking core reaction model is based.

Provided activation energies were obtained for rate constant K_1 and effective diffusion coefficient D_e, numerical solutions could be obtained to predict the weight loss of organic vehicle under non-isothermal conditions. The shrinking core reaction model can be applied to flat plates, cylinders and spheres and most moulded parts can be approximated as composites of these shapes.

4. Conclusions

By applying shrinking unreacted core reaction kinetics to the isothermal removal of organic vehicles from injection-moulded ceramic bodies, it is shown that diffusion rather than reaction rate controls the weight loss in the presence of oxygen. An effective diffusion coefficient is obtained which is likely to reflect the outward diffusion of reaction products rather than oxygen diffusion in the molten polymer. The appearance of surface bloating in some samples caused by degradation products despite the low temperature of study confirms this. Although the presence of oxygen causes enhanced removal of organic vehicle from the surface, low temperatures would be needed to increase the ratio of oxidative to thermal degradation reaction rates. Predicted times for complete removal of organic vehicle from 2 mm thick discs under isothermal conditions at 180 °C are as high as 135 days. The prospects of securing complete removal of organic vehicle from large mouldings by a surface reaction without internal thermal degradation are bleak. The shrinking unreacted core model does provide a method for the quantitative analysis of the oxidation of organic vehicle in ceramic bodies, and numerical solutions to the non-isothermal problem could be developed.

Acknowledgements

The authors are grateful for SERC funding for the Ceramic Injection Moulding Programme and to Professor B. Rand for helpful discussions.

References

1. M. J. EDIRISINGHE and J. R. G. EVANS, *Int. J. High Tech. Ceram.* **2** (1986) 1.
2. *Idem., ibid.* **2** (1986) 249.
3. E. WAINER, US Patent 2 593 507 (1952).
4. US Patent 706 728 (1954), assigned to Bendix Aviation Corporation.
5. K. SAITO, T. TANAKA and T. HIBINO, UK Patent 1 426 317 (1976), assigned to Tokyo Shibaura Electric Co. Ltd.
6. A. M. LITMAN, N. R. SCHOTT and S. W. TOZLOWSKI, *Soc. Plast. Eng. Tech.* **22** (1976) 549.

7. A. JOHNSSON, E. CARLSTROM, L. HERMANSSON and R. CARLSSON, *Proc. Br. Ceram. Soc.* **33** (1983) 139.
8. N. GRASSIE, in "Macromolecular Science", MTP International Review of Science, Physical Chemistry Series One, Vol. 8, edited by C. E. M. Bawn (Butterworths, London, 1972) pp. 277–328.
9. Y. TSUCHIYA and K. SUMI, *J. Polym. Sci. A-1* **6** (1968) 415.
10. N. GRASSIE and A. SCOTNEY, in 'Polymer Handbook', 2nd Edn, edited by J. Brandrup and E. M. Immergut (Wiley, New York, 1975) p. II, 467.
11. J. K. WRIGHT, J. R. G. EVANS and M. J. EDIRISINGHE, *J. Amer. Ceram. Soc.* **92** (1989) 1822.
12. J. K. WRIGHT, M. J. EDIRISINGHE, J. G. ZHANG and J. R. G. EVANS, *J. Amer. Ceram. Soc.* **73** (1990) 2653.
13. C. L. QUACKENBUSH, K. FRENCH and J. T. NEIL, *Ceram. Eng. Sci. Proc.* **3** (1982) 20.
14. J. G. ZHANG, M. J. EDIRISINGHE and J. R. G. EVANS, *Industr. Ceram.* **9** (1989) 72.
15. M. J. EDIRISINGHE and J. R. G. EVANS, *Br. Ceram. Trans. J.* **86** (1987) 18.
16. J. SZEKELY, J. W. EVANS and H. Y. SOHN, "Gas–Solid Reactions" (Academic, New York, 1976) pp. 65–107.
17. S. L. MADORSKY, *J. Polym. Sci.* **9** (1952) 133.
18. O. S. ÖZGEN and B. RAND, *Br. Ceram. Trans. J.* **84** (1985) 70.
19. *Idem., ibid.* **84** (1985) 213.
20. T. H. MELTZER, J. J. KELLEY and R. N. GOLDEY, *J. Appl. Polym. Sci.* **3** (1960) 84.
21. I. MITA and K. HORIE, in "Degradation and Stabilization of Polymers", edited by H. H. G. Jellinek (Elsevier, Amsterdam, 1983) p. 278.
22. L. REICH and S. S. STIVALA, "Autooxidation of Hydrocarbons and Polyolefins" (Dekker, New York, 1969) pp. 462–470.
23. R. M. BARRER, in "Diffusion of Polymers", edited by J. Crank and G. S. Park (Academic, London, 1968) p. 165.
24. D. BEDEAUX and R. KAPRAL, *J. Chem. Phys.* **79** (1983) 1783.
25. S. SRIDHARAN and R. I. CUKIER, *J. Phys. Chem.* **91** (1987) 2962.
26. "Handbook of Chemistry and Physics", 55th Edn, edited by R. C. Weast (CRC Press, Cleveland, Ohio, 1974) p. F215.
27. Loc. cit. 22, pp. 42–48.
28. Loc. cit. 22, p. 464.

Received 30 April
and accepted 19 November 1990